Appl Nanosci (2014) 4:1013–1019
DOI 10.1007/s13204-013-0284-z

ORIGINAL ARTICLE

Synthesis and structural, optical and thermal properties of CdS:Zn^{2+} nanoparticles

S. Muruganandam · G. Anbalagan · G. Murugadoss

Received: 4 May 2013 / Accepted: 16 November 2013 / Published online: 4 December 2013

Abstract Undoped and Zn (1–5, 10 %) -doped CdS nanoparticles were successfully synthesized by chemical method and polyvinylpyrrolidone was used as capping agent. The morphology and crystalline structure of the samples were studied by transmission electron microscopy and X-ray diffraction. The average particle size of the spherical nanoparticles determined by these techniques was of the order of 2.5–6 nm. The functional groups of the capping agent on CdS:Zn^{2+} surface were identified by FT-IR study. The band gap of the nanoparticles was calculated using UV–visible absorption spectra and the result showed that the band gap values were dramatically blue shifted from the bulk CdS. The optimum concentration of the doping ions was selected through absorption study. Photoluminescence of the CdS:Zn^{2+} nanoparticle showed strong blue and green emission. The thermal properties of the nanoparticles were analyzed by thermogravimetric-differential thermal analysis.

Keywords CdS · Nanoparticles · Chemical method · XRD · Photoluminescence

Introduction

In recent years, semiconductor nanoparticles have received broad attentions because of their interesting and novel electronic, thermoelectronic and optical properties intrinsically associated with their low dimensionality and the quantum confinement effect (Pan et al. 2001; Duan et al. 2003; Murugadoss 2014). The properties of nanostructured materials are highly affected by the physical parameters that include size, shape, composition, crystallinity and microstructure (Seoudi et al. 2010; Chawla Puja et al. 2010). CdS is an important semiconductor compound of the II–VI group with excellent physical properties and band gap energy of 2.42 eV. It has been extensively studied due to its potential application in field effect transistor, light-emitting diodes, photocatalysis, biological sensors, solar cells and photodegradation of water pollutants (Alivisatos 1996; Colvin et al. 1994; Klein et al. 1997; Ruxandra and Antohe 1998; Romeo et al. 2010; Beecroft and Ober 1997). The electronic properties of CdS nanoparticles doped with transition metals are strongly influenced by the doped transition metals (Liu Kewei et al. 2007). Wageh and Badr (2008) have reported that the $Cd_{1-x}Zn_xS$ nanoparticle is stabilized by the bifunctional organic molecule. Unni (2009) has reported on the size-tunable aqueous synthesis and PL properties of the Zn^{2+}- and Cu^{2+}-doped CdS nanophosphors. There have been only a few reports on Zn^{2+}-doped CdS nanoparticles (Wang et al. 2010; Zhang et al. 2007; Xing et al. 2006; Wang et al. 2012). Transition metals doped with CdS nanoparticles with good structural, magnetic and optical qualities have been reported from a variety of techniques such as surfactant-assisted synthesis, chemical precipitation method, spray pyrolysis, ion implantation and high-energy electron irradiation. In this work, we used the chemical precipitation method. It is the most popular technique that is used in industrial applications because of the cheap raw materials, easy handling and large-scale production (Souici et al. 2006). To improve the uniformity and capability of CdS:Zn nanoparticle, it is

S. Muruganandam · G. Anbalagan (✉)
Department of Physics, Presidency College, Chennai 600 005, Tamilnadu, India
e-mail: anbu24663@yahoo.co.in

G. Murugadoss
Centre for Nanoscience and Technology, Anna University, Chennai 600 025, Tamilnadu, India

capped with water-soluble polyvinyl pyrrolidone (PVP). Through the surface modification with PVP, highly monodispersed CdS nanoparticles were prepared, which exhibited significantly enhanced luminescence and high chemical stability.

Experimental

Materials

To synthesize Zn-doped CdS, the following materials were used. The chemical reagents used were of analytical reagent grade without further purification. Cadmium acetate ($Cd(CH_3COO)_2.2H_2O$), zinc acetate ($Zn(CH_3COO)_2.4H_2O$) and sodium sulfide ($Na_2S.xH_2O$) obtained from Nice Chemical Company were used as precursors. Polyvinyl pyrrolidone (PVP 40,000) was obtained from Aldrich. All the chemicals were above 99 % purity. All the glassware used in this experimental work were acid washed. Ultrapure water was used for all dilution and sample preparations.

In a typical experiment, 2.66 g of cadmium acetate in 100 ml deionised water was mixed with 25 ml of zinc acetate (1–5 and 10 %) solution. The mixture was stirred magnetically at 80 °C until a homogeneous solution was obtained. Then, 1.1 g (0.1 M) of 100 ml Na_2S was added drop by drop to the above mixture. After the Na_2S injection, a yellow voluminous precipitate appeared. It slowly dissolves under formation of CdS:Zn^{2+} nanoparticles under stirring for 30 min at 120 °C. The obtained yellow color colloidal solution was purified by dialysis against de-ionized water and acetone several times to remove impurities. The products were dried in a hot air oven at 80 °C for 2 h. In addition, for synthesis of surfactant (PVP) capped particles, different amounts (0.5–2.5 g) of PVP were added to cadmium acetate solution before the addition of zinc acetate.

Characteristic techniques

The synthesized nanoparticles were characterized using the following techniques: X-ray diffraction (XRD) pattern was collected on an X'Pert PRO diffractometer with Cu Kα radiation (λ = 1.54066 Å). Transmission electron microscopy (TEM) was performed using HITACHI (Japan) H–7650, 100 kV. The formations of nanoparticles were studied using Fourier transfer infrared spectroscopy (FT-IR) NICOLET AVATAR 3330. The UV–visible absorption spectrum was recorded using a Varian incorporates (U.S) Cary 500 UV–visible spectrometer. Room temperature photoluminescence phenomenon of the samples was studied on Cary-Eclipse spectrometer. Thermal analysis including TGA and DTA was carried out using a simultaneous thermal analyzer SDT Q600 V8.3 Build 101, heating rate 20 °C/min in air atmosphere.

Results and discussion

Structural and morphological study

Figure 1 shows the XRD pattern of undoped, Zn^{2+}- (1–5 and 10 %) doped and PVP-capped CdS nanoparticles. The XRD peaks are found to be very broad indicating very fine

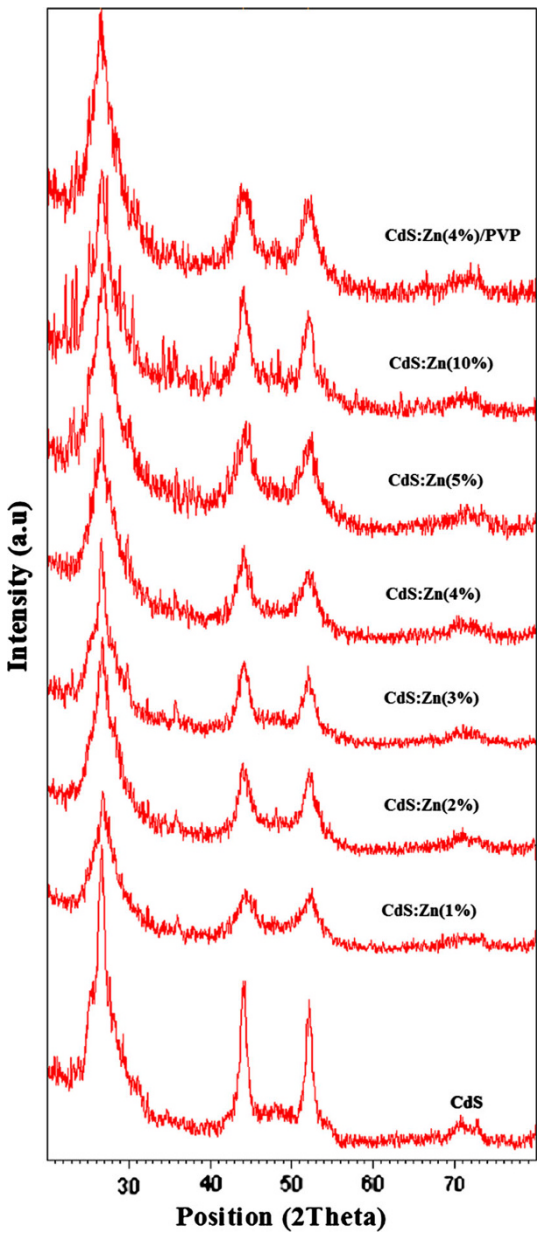

Fig. 1 XRD patterns of the undoped CdS, doped CdS:Zn^{2+} (1–5 and 10 %) and PVP-capped CdS:Zn^{2+} (4 %) nanoparticles

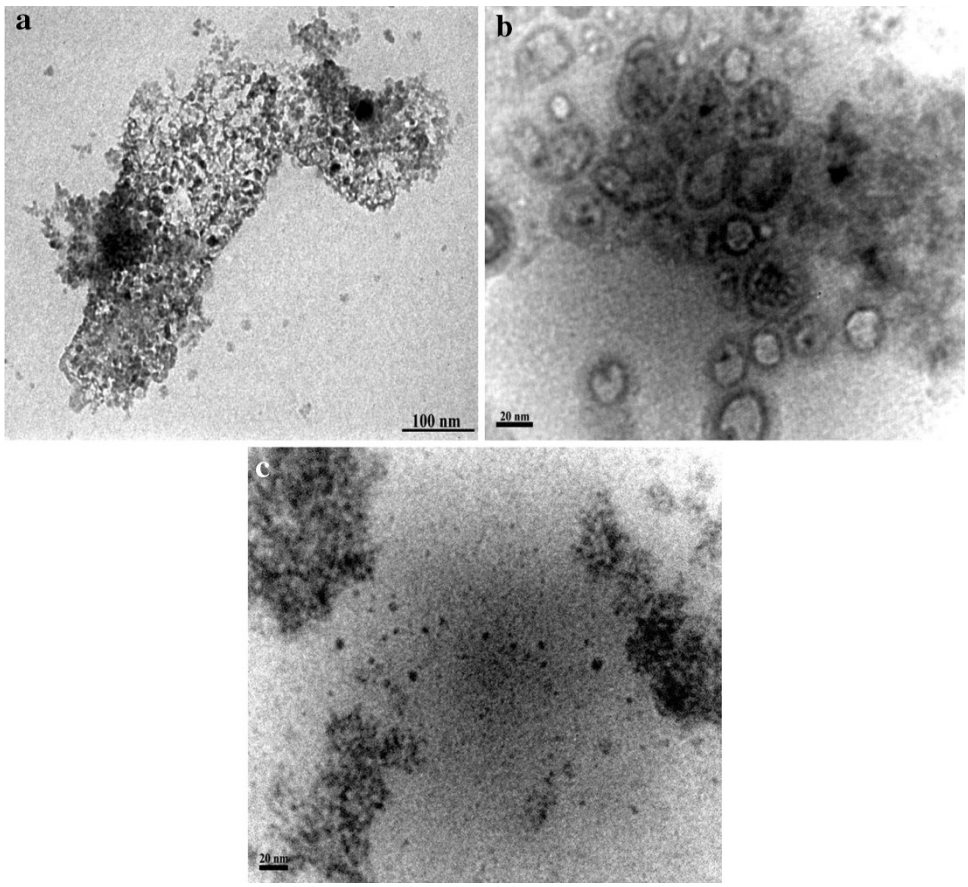

Fig. 2 TEM images show **a** undoped CdS, **b** doped CdS:Zn^{2+} (4 %) and **c** CdS:Zn^{2+} (4 %)/PVP-capped nanoparticles

size of the grains. The XRD pattern exhibits prominent broad peaks at $2\theta = 26.5°$, 43.9° and 52.1° which could be indexed to diffraction from the (1 1 1), (2 2 0) and (3 1 1) planes of cubic CdS, according to JCPDS file (JCPDS no. 10–454). It can be seen that the peak position of the doped samples is not changed with respect to doping (Zn^{2+}) concentrations.

However, the relative intensity is varied. The peak broadness of the surfactant-capped nanoparticles shows decrease in size than that of the free-surfactant particles. It depicts the role of the surfactant in this research work. The average grain size was calculated using Scherrer's formula (Murugadoss et al. 2010).

$$D = k\lambda/\beta \cos\theta \quad (1)$$

where k is particle shape factor (taken as 0.94), λ is the X-ray wavelength (0.1542 nm), β is full width at half maximum (FWHM) and θ is the diffraction angle in degrees (half of the peak position angle). According to the calculation, the average grain size of undoped CdS nanoparticles is 4.5 nm. The size of the Zn^{2+}-doped (4 %) and PVP-capped CdS:Zn^{2+}(4 %) nanoparticles is 3.4 and 2.8 nm, respectively. Figure 2a, b shows TEM images of the pure CdS and doped CdS:Zn^{2+}(4 %) nanoparticles aggregated with a size of 4.5 and 3.5 nm, respectively. As shown in Fig. 2a, the particles are spherical in shape.

However, the Zn (4 %) -doped CdS (Fig. 2b) nanoparticles showed as core–shell structure. The PVP-capped CdS:Zn^{2+} (Fig. 2c) shows that the particles are well dispersed with an estimated particle size of about 3.0 nm. These values are consistent with the results obtained from X-ray diffraction. From the TEM photographs, one can find that PVP played an important role in controlling the size of CdS:Zn^{2+}.

FT-IR study

FT-IR spectra of pure CdS, CdS:Zn^{2+} (1–5 and 10 %) -doped and PVP-capped CdS:Zn^{2+} (4 %) nanoparticle are shown in Fig. 3a–h. The presence of strong absorption band in the region between 600 and 700 cm^{-1} is due to Cd–S stretching vibration (Martin and Schaber 1982). The absorption peak occurs at 927 cm^{-1} due to S–O stretching vibration. The weak absorption band appeared at 1,110 cm^{-1} due to Zn–S stretching mode, and may be due to some amount of Cd^{2+} replaced by Zn^{2+} ions (Murugadoss 2010). The weak peaks at 2,360, 2,343 and 1,645 cm^{-1}, attributed to microstructure formation, may be present in the samples. The strong peaks appearing at 3,433

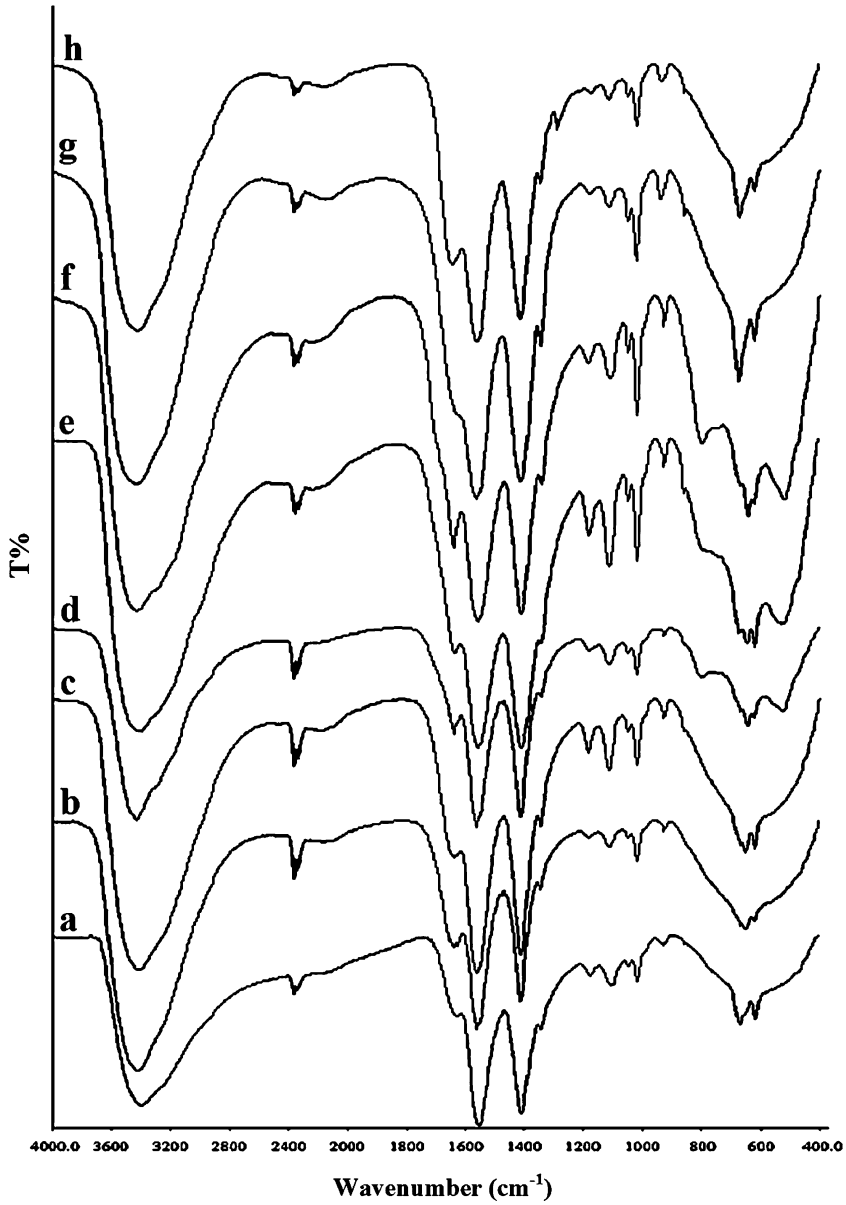

Fig. 3 FT-IR spectra show **a** undoped CdS, **b–g** doped CdS:Zn^{2+}(1–5 and 10 %) and **h** CdS:Zn^{2+}(4 %)/PVP-capped nanoparticles

and 1,560 cm^{-1} are due to O–H stretching vibration and CO_2 adsorbed on the surface of the particles, respectively. In fact, adsorbed water and CO_2 are common to all samples exposed to the atmosphere. As shown in Fig. 3h, the peak appeared at 1,290 cm^{-1} due to C–O stretching vibration. It shows the presence of PVP on the CdS:Zn^{2+} surface.

Optical study

Figure 4 shows UV–visible absorption spectra of undoped CdS:Zn^{2+}(1–5 and 10 %) and PVP-capped CdS:Zn^{2+} nanoparticle in the range of 400–700 cm^{-1}. The absorption values of all samples were blue shifted from bulk CdS. Similar result was observed by Unni et al., for Zn^{2+} (5 %) - doped CdS nanoparticle. This result is a direct consequence of the quantum conferment effect, due to the decrease in particle size (Brus 1984). The band gap of the samples was determined by the following equation (Chowdhury et al. 2005) and presented in Table 1:

$$E_{gn} = hc/\lambda_e \quad (2)$$

Using the calculated band gap value, the average particle size was measured by Brus formula (Brus 1984).

$$E_{np} = E_g + \hbar\pi^2/2R^2\left[1/m_e^* + 1/m_h^*\right] - 1.8e^2/4\pi\varepsilon_0\varepsilon_r R \quad (3)$$

where E_{np} is the band gap of the nanoparticles, E_g is the band gap of bulk CdS (2.42 eV), m_e* is the effective mass of the electron (0.19 m_o), m_h* is the effective mass of the hole (0.8 m_o), m_o is the rest mass of electron, R is the radius of the particle, ε_r is dielectric constant (5.7), ε_o

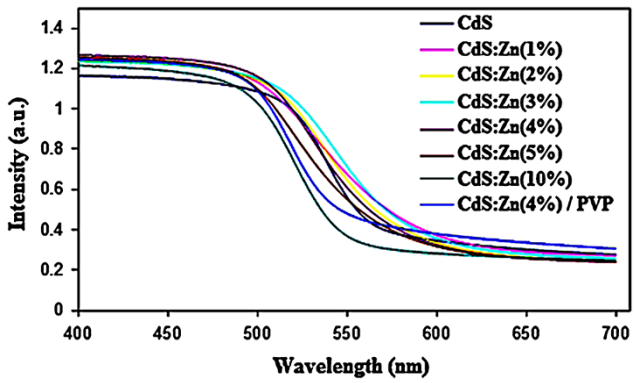

Fig. 4 UV–Vis absorption spectra of undoped CdS, doped CdS:Zn^{2+} (1–5 and 10 %) and CdS:Zn^{2+} (4 %)/PVP-capped nanoparticles

Table 1 Energy gap, absorption and particle size of undoped, doped and PVP-capped CdS: Zn^{2+}(4 %) nanoparticles

Doping concentration	Band gap (E_{gn}) eV	Absorption wavelength (nm)	UV–Vis particle size (nm)	XRD particle size (nm)	TEM particle size (nm)
CdS	2.60	478	4.4	4.5	4.5
CdS: Zn^{2+}(4 %)	2.73	454	3.3	3.4	3.5
CdS:Zn^{2+}(4 %)/ PVP	2.78	447	3.0	2.8	3.0

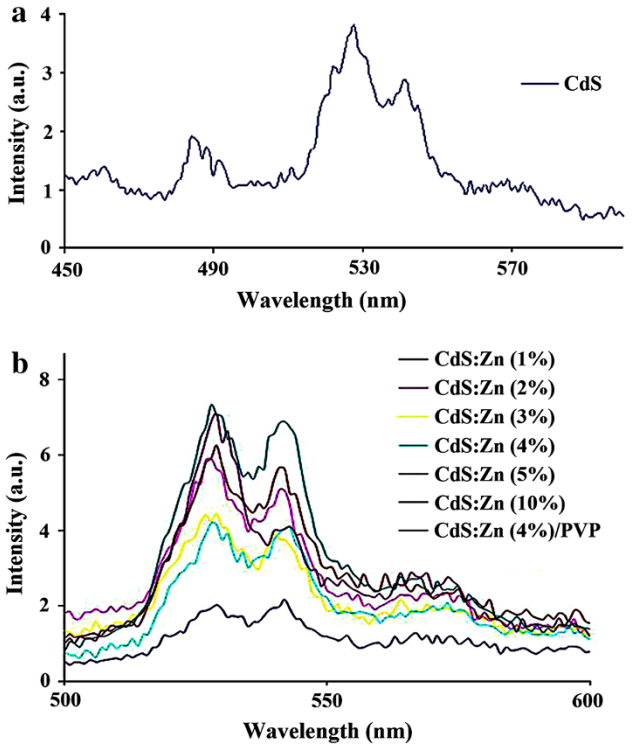

Fig. 5 **a** Photoluminescence spectra of the CdS nanoparticles, **b** CdS:Zn^{2+}(1–5 and 10 %) and CdS:Zn^{2+}(4 %)/PVP-capped nanoparticles

is the permittivity of free face and 'e' is the charge of electron.

As shows in Table 1, the particle sizes are decreased by increasing the band gap values. This absorption shift is due to the quantum size effect, representing a change in band gap along with exciton features, which can be used as a measure of particle size and size distribution (Beecroft and Ober 1997). The calculated particle sizes are in good agreement with the XRD and TEM results (Table 1).

The PL spectra of synthesized nanoparticles recorded at room temperature for different absorption values are presented in Fig. 5. Figure 5a, b shows the PL spectrum of undoped CdS and Zn^{2+} (1–5 and 10 %) -doped CdS and PVP-capped CdS:Zn^{2+} nanoparticle, respectively. The PL spectrum is observed to be broad in the visible region.

In addition, the peak positions of the doped samples are slightly shifted with respect to the doping concentrations as shown in Fig. 5b. The broad PL spectrum is due to trap state emissions arising from surface defect states (Saunders et al. 2006). When CdS nanoparticles absorb photons, the electrons are excited from valence band to the conduction band and are trapped by defects. The recombination of the defects and excitation states induced by Zn^{2+} provides modified surface trap states, which enhance and shift the luminescence band (Yang et al. 2002). Both samples (undoped and doped CdS) are found to exhibit strong emission bands at 527 and 542 nm in the visible region. The peak position of PL spectra is nearly same for all the samples. However, the relative intensities were changed. The emission peak of the PVP-capped CdS:Zn^{2+} nanoparticle is more enhanced than the uncapped particles. It shows that PVP is not only used to control the particle size, but also to reduce the surface defects. Enhanced PL emission is observed for the PVP-capped CdS:Zn^{2+} nanoparticles as shown in Fig. 5b.

Thermal study

Thermogravimetric (TG) and differential thermal analysis (DTA) were used to study the thermal decomposition of undoped and Zn^{2+}-doped CdS nanoparticles. The synthesized specimens were heated from room temperature to 1,000 °C with an increment of 20 °C/min in air. The combined plots of TG and DTA curves show the undoped (Fig. 6a) and Zn^{2+} (4 %) -doped CdS (Fig. 6b) nanoparticles. From TG data plots, it is noticed that the weight loss of the nanoparticles is found to take place up to 800 °C. The weight loss of TG curves of both the samples up to 100 °C mainly corresponds to evaporation of water, residual solvent and organic molecules.

The DTA curve of Fig. 6a shows a strong exothermic peak at 328 °C, probably corresponding to the lattice

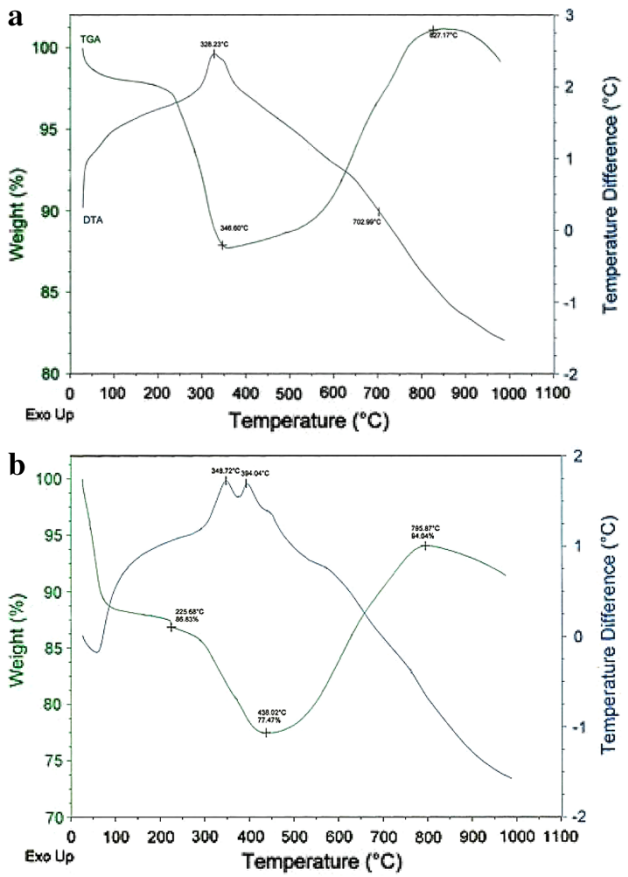

Fig. 6 **a** TG and DTA curves of undoped CdS nanoparticles and **b** CdS:Zn^{2+} (4 %) nanoparticles

deformation of CdS or release of sulfur ion from CdS. In addition, two exothermic peaks were observed at 348 and 394 °C for Zn-doped CdS nanoparticles (Fig. 6b). It may be due to sequential events of the lattice deformation and release of the dopant ion, respectively. The corresponding weight loss is observed as shown in Fig. 6a, b in TG curves. On further increasing the temperature (>400 °C), a significant weight gain is observed at 850 °C for CdS and 800 °C for CdS:Zn as shown in the TGA curves (Fig. 6a, b). These may be due to oxidation of the cadmium ions in the air atmosphere.

Conclusions

CdS and CdS:Zn nanoparticles are potential candidate for various applications like optoelectronic devices and solar cells; hence, they were studied in the present work. TEM results showed that the synthesized particles were spherical in shape with 2.5–6 nm range size. The presence of the capping agent (PVP) on CdS:Zn was identified through FT-IR. The position of the absorption peaks was shifted toward higher energy with a decrease in the nanoparticles size. The optimum concentration of the doping ion was selected as 4 % by optical study. Thermal stability and decomposition of the CdS and Zn-doped CdS nanoparticles were discussed by TG-DTA analysis.

References

Alivisatos AP (1996) Semiconductor clusters, nanocrystals, and quantum dots. Science 271:933–937

Beecroft LL, Ober CK (1997) Nanocomposite materials for optical applications. Chem Mater 9:1302–1317

Brus LE (1984) Electron–electron and electron-hole interactions in small semiconductor crystallites: the size dependence of the lowest excited electronic state. J Chem Phys 80:4403–4409

Chowdhury S, Ahmed GA, Mohanta D, Dolui SK, Avasthi DK, Choudhury A (2005) Luminescence study of bare and coated CdS quantum dots: effect of SHI irradiation and ageing. Nucl Instr Meth Phys Res B 240:690–696

Colvin VL, Schlamp MC, Alivisatos AP (1994) Light-emitting diodes made from cadmium selenide nanocrystals and a semiconducting polymer. Nature 370:354–357

Duan XF, Huang Y, Agarwal R, Lieber CM (2003) Single nanowire electrically driven lasers. Nature 421:241–245

Kewei L, Zhang JY, Xiaojie W, Li B, Li B, Youming L, Fan X, Shen D (2007) Fe-doped and (Zn, Fe) co-doped CdS films: could the Zn doping affect the concentration of Fe and the optical properties? Physica B 38:248–251

Klein DL, Roth R, Lim AKL, Alivisatos AP, McEuen PL (1997) A single-electron transistor made from a cadmium selenide nanocrystal. Nature 389:699–701

Martin TP, Schaber H (1982) Matrix isolated II-VI molecules: sulfides of Mg, Ca, Sr, Zn and Cd. Spectrochem Acta A 38:655–660

Murugadoss G (2010) Synthesis and optical characterization of PVP and SHMP-encapsulated Mn^{2+}-doped ZnS nanocrystals. J Lumin 130:2207–2214

Murugadoss G (2014) Synthesis and study of optical and thermal properties of multi layers coated CdS core–shell nanocomposites. J Lumin 146:430–434

Murugadoss G, Rajamannan B, Ramasamy V (2010) Synthesis, characterization and optical properties of water-soluble ZnS:Mn^{2+} nanoparticles. J Lumin 130:2032–2039

Pan ZW, Dai ZR, Wang ZL (2001) Nanobelts of semiconducting oxides. Science 291:1947–1949

Puja C, Lochab SP, Singh N (2010) Photoluminescence, thermoluminescence and Raman studies of CdS nanocrystalline phosphor. J Alloy Comp 492:662–666

Romeo N, Bosio A, Romeo A (2010) An innovative process suitable to produce high-efficiency CdTe/CdS thin-film modules. Solar Energy Mater Soller Cells 94:2–7

Ruxandra V, Antohe S (1998) The effect of the electron irradiation on the electrical properties of thin polycrystalline CdS layers. J Appl Phys 84:727–733

Saunders AE, Popov I, Banin U (2006) Synthesis of hybrid CdS−Au colloidal nanostructures. J Phys Chem B 110:25421–25429

Seoudi R, Shabaka A, Eisa WH, Anies B, Farage NM (2010) Effect of the prepared temperature on the size of CdS and ZnS nanoparticle. Physica B 405:919–924

Souici AH, Keghouche N, Delaire JA, Remita H, Mostafavi M (2006) Radiolytic synthesis and optical properties of ultra-small stabilized ZnS nanoparticles. Chem Phys Lett 422:25–29

Unni C, Philip D, Smitha SL, Nissamudeen KM, Gopchandran KG (2009) Aqueous synthesis and characterization of CdS, CdS:Zn^{2+} and CdS:Cu^{2+} quantum dots. Spectrrochimica Acta Part A 72:827–832

Wageh S, Badr MH (2008) $Cd_{1-x}Zn_xS$ nanoparticles stabilized by a bifunctional organic molecule. Physica E 40:2810–2813

Wang L, Wang W, Shang M, Yin W, Sun S, Zhang L (2010) Hydrothermal synthesis of monodisperse ZnxCd1-xS spheres and their photocatalytic properties. Int J Hydrogen Energy 35:19–25

Wang J, Li B, Chen J, Li N, Zheng J, Zhu Z (2012) Enhanced photocatalytic H2- production activity of CdxZn1-xS nanocrystals by surface loading MS (M = Ni Co., Cu) species. Appl Surf Sci 259:118–123

Xing C, Zhang Y, Yan W, Guo L (2006) Band structure-controlled solid solution of Cd1- xZnxS photocatalyst for hydrogen production by water splitting. Int J Hydrogen Energy 31:2018–2024

Yang P, Lu MK, Song CF, Xu D, Yuan DR, Cheng XF, Zhou GJ (2002) Luminescence of Cu^{2+} and In^{3+} co-activated ZnS nanoparticles. Opt Mater 20:141–145

Zhang K, Jing D, Xing C, Guo L (2007) Significantly improved photocatalytic hydrogen production activity over Cd1-xZnxS photocatalysts prepared by a novel thermal sulfuration method. Int J Hydrogen Energy 32:4685–4691